Ann. occup. Hyg., Vol. 46, No. 8, pp. 663–672, 2002
Published by Oxford University Press
DOI: 10.1093/annhyg/mef089

Investigation of the Aerosols Produced by a High-speed, Hand-held Grinder Using Various Substrates

ANTHONY T. ZIMMER* and ANDREW D. MAYNARD

National Institute for Occupational Safety and Health, Division of Applied Research and Technology, 4676 Columbia Parkway, Cincinnati, OH 45226, USA

Received 2 April 2002; in final form 22 July 2002

Mechanical processes such as grinding are classically thought to form micrometer scale aerosols through abrasion and attrition. High-speed grinding has been used as the basis for testing the hypothesis that ultrafine particles do not form a substantial component of mechanically generated aerosols. A wide variety of grinding substrates were selected for evaluation to represent the broad spectrum of materials available. To characterize the particle size distribution over particle sizes ranging from 4.2 nm to 20.5 μm, the aerosol-laden air collected from an enclosed chamber was split and directed to three aerosol instruments operated in parallel. Transmission electron microscope samples of the various grinding substrates were also collected. The results demonstrate that ultrafine particles do have the potential to form a significant component of a grinding aerosol for a number of substrates. It appears that the ultrafine aerosols were formed by the following processes: (i) from within the grinding motor, (ii) from the combustion of amenable grinding substrates and (iii) from volatilization of amenable grinding materials at the grinding wheel/substrate interface.

Keywords: grinding; particle size distribution; ultrafine aerosols

INTRODUCTION

It is generally assumed that aerosols generated during mechanical processes such as grinding are characterized by large particles formed through attrition. Consequently, little attention has been given to the generated particle concentration much below 1 μm. While it is conceivable that the mass-weighted distribution of such aerosols may be dominated by supermicrometer particles, it is by no means clear that the same will apply for particle number- and surface area-weighted distributions. Recent published research has indicated that for some classes of material (notably materials leading to aerosol particles with low solubility) biological activity following inhalation may be more appropriately represented by aerosol number or surface area concentration (Oberdorster *et al.*, 1995; Donaldson *et al.*, 1998; Brown *et al.*, 2001). As the particle number or surface area per unit mass increases with decreasing particle size within an aerosol, the presence of submicrometer particles becomes increasingly significant as exposure metrics other than mass are considered. Indeed, much of the current discussion surrounding the toxicity of low-solubility particles traditionally considered to be chemically inert has focused on particles <100 nm in diameter; commonly termed ultrafine particles.

Very little attention has been given to the possibility of mechanical generation leading to substantial aerosol exposure from ultrafine particles. Limited data indicate that it is possible to generate high particle number concentrations from mechanical processes. McCawley *et al.* (2001) have shown that the number-weighted aerosol size distribution generated while grinding beryllium ceramic is dominated by particles <100 nm and Choe *et al.* (2000) have shown that dry paint scraping and sanding can lead to substantial particle number concentrations below 1 μm. However, apart from these studies there is little in the literature to indicate the likely contribution of mechanical processes to ultrafine aerosols in the workplace.

Grinding represents a typical mechanical operation found in many workplaces. Weight-based (e.g. gravimetric) sampling is typically conducted to characterize grinding operations (Lehmann and Frohlich, 1988; Thorpe and Brown, 1994) for comparison with

*Author to whom correspondence should be addressed.
Tel: +1-513-841-4370; fax: +1-513-841-4545;
e-mail: azimmer@cdc.gov

various exposure criteria (ACGIH, 1990; NIOSH, 1992; OSHA, 1997). Due to the assumption that the aerosols generated from these processes mainly result from mechanical attrition of the substrate, prior research to characterize the particle size distribution has focused upon the micrometer size regime using techniques such as cascade impaction (Lehmann and Frohlich, 1988; Kusaka *et al.*, 1992).

Grinding typically occurs on a wide variety of substrates. Some substrates have no specific exposure criteria and are evaluated as a 'particulate not otherwise regulated' with exposure limits ranging from 5 to 15 mg/m^3 for respirable and total exposure, respectively (OSHA, 1997). Other substrates, such as wood dusts and metals, can be evaluated and compared with specific exposure criteria. Interestingly, metals such as aluminum and copper have exposure criteria that are lower for the metal fume than the metal dust (i.e. method of generation) (ACGIH, 1990; OSHA, 1997).

In this study, high-speed grinding was used to test the hypothesis that ultrafine particles do not form a substantial component of mechanically generated aerosols. Aerosols from the grinder were produced in a controlled environment, using a variety of grinding substrates, and the grinding aerosol was characterized over a particle size range from 4.22 nm to 20.5 μm.

MATERIALS AND METHODS

HEPA-filtered, particle-free air was pulled upward through a stainless steel chamber (0.914 m long, 0.813 m wide, 1.19 m tall) using a commercially available, industrial air cleaner (model 73-800G; ACE Corp., St Louis, MO) (Fig. 1). Prior to measurements, the air cleaner was turned on and the HEPA-filtered air within the chamber was monitored using a condensation particle counter (CPC) (model 3022A; TSI Inc., Shoreview, MN). When the particle number concentration was reduced to a value of ~50 particles/cm^3, the air cleaner was turned off to prevent flow through the chamber. A small, tubeaxial fan (model 8500C; Pamotor, Burlingame, CA), located within the chamber, was used to create 'stirred' conditions within the chamber (CPC measurements validated that the fan did not represent a source of aerosols within the chamber).

Grinding was accomplished using a Multipro™ (model 395; Dremel, Racine, WI), a variable speed tool with rotational speeds that can be varied from 5000 to 30000 r.p.m. A cylindrical grinding wheel, composed of sintered aluminum oxide, was selected for these experiments (diameter 1.6 cm, length 1.0 cm). To prevent cross-contamination, new grinding wheels were used for each substrate tested. The rotational speed of the grinding wheel was determined using a tachometer (Dynapar model HT50; Danaher Controls, Gurnee, IL). Grinding was accomplished such that the cylindrical wheel was placed normal to the substrate with a constant applied force of 3.96 N. A wide variety of grinding substrates were selected for evaluation to represent the broad spectrum of materials available. The substrates selected included both relatively homogeneous and heterogeneous materials

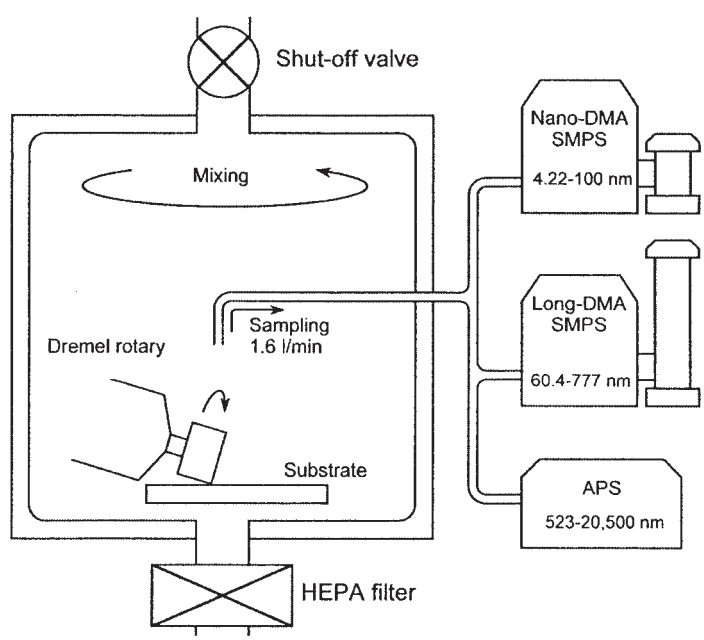

Fig. 1. Schematic of the grinding generation and aerosol sampling apparatus. Note that the shut-off valve closed when generating and sampling grinding aerosols.

and included steel, aluminum, polytetrafluoroethylene (PTFE), hardwood, granite and clay ceramic.

A number of aerosol instruments were used to evaluate the aerosol behavior and the resultant particle size distribution during a grinding operation. Using stainless steel and flexible graphite tubing to attenuate charging effects within the sample line, the grinding aerosols were collected from the stainless steel chamber from a position located directly above the grinding operation (height 15 cm). To ensure that there was little temporal variation over the time scales needed to collect aerosol samples, a CPC was used to characterize the temporal variation of the total number concentration during a grinding sample run.

To characterize the particle size distribution, the aerosol-laden air from the chamber was split and directed to three aerosol instruments operated in parallel. Small, nanometer scale particles [4.22 nm < d_p (particle diameter) < 100 nm] were characterized using a scanning mobility particle sizer (SMPS) configured with a nano differential mobility analyzer (DMA) (electrostatic classifier model 3080 using a DMA model 3085 and a condensation particle counter model 3022A; TSI Inc., St Paul, MN). Larger, nanometer scale particles (60.4 nm < d_p < 777 nm) were characterized using a SMPS configured with a long DMA (DMA model 3934 and a condensation particle counter model 3022A; TSI Inc.). Larger, primarily micrometer scale particles (523 nm < d_p < 20.5 μm) were characterized using an aerodynamic particle sizer (APS) (model 3320; TSI Inc.). Rogak *et al.* (1993) have shown particle mobility diameter to agree well with equivalent-sphere projected area diameter for fractal-like particles <1 μm. The assumption was therefore made that the data from each SMPS could be interpreted in terms of particle equivalent-sphere projected area diameter. Particles large enough to be sampled by the APS were assumed to arise predominantly through attrition and therefore to have a compact morphology. APS aerosol size distributions were therefore transformed to particle number concentration versus equivalent-sphere projected area diameter assuming spherical particles with the same density as the bulk substrate material. Furthermore, the APS data were corrected for sampling train losses between the chamber and the instrument inlet and losses within the APS nozzle (Kinney and Pui, 1995). Calculations indicated sampling train losses to each SMPS to be negligible. The total sample time for each SMPS measurement was 230 s (up-scan time 200 s, down-scan time 30 s) while the total sample time for each APS measurement was 200 s.

Transmission electron microscope (TEM) samples of the aerosol generated from each substrate type were also collected using a point-to-plane electrostatic precipitator (Cheng *et al.*, 1981).

Triplicate, randomized samples were obtained for each grinding substrate. During a typical experimental sample run, the grinding substrate was attached to a holder. The grinding wheel was placed on the substrate and the grinding speed was adjusted to 20000 r.p.m. using a rheostat (model 3PN751; Matheson Scientific) and a tachometer. The chamber was HEPA filtered to remove aerosols within the chamber and the ventilation system was turned off. After ~30 s, grinding was conducted on the substrate for 10 s, ensuring that the aerosol number concentration was sufficiently low to suppress coagulation dynamics (typical number concentrations were $<10^6$ particles/cm^3). Simultaneous aerosol sampling (i.e. SMPS/NDMA, SMPS/LDMA and APS) was started 60 s after the grinding burst. Sampling was started at this point, based upon CPC measurements suggesting that the aerosol within the chamber was well mixed and that the particle number concentration did not vary appreciably over the necessary time scales.

To ensure that the aerosols measured representative products of grinding, background aerosol measurements were also taken with the grinding tool freely spinning within the chamber at 20000 r.p.m. with an unused sintered aluminum oxide grinding wheel. Given the unlikely probability that aerosols were created from the grinding wheel, this measurement represented the aerosols produced primarily by the grinding tool motor. This result was subtracted from measured size distributions for each grinding substrate.

RESULTS

The aerosol produced solely by the grinding tool and the background corrected measurements for each of the substrates are presented in Fig. 2a–g, with electron micrographs of representative particles shown in Fig. 3a–e. In many cases the measured size distributions exhibited multi-modal behavior. The measurements obtained using each aerosol instrument are represented by different symbols (i.e. solid circles for the SMPS/NDMA configuration, hollow circles for the SMPS/LDMA configuration and solid triangles for the APS). Each point in the figures represents the arithmetic mean of the triplicate random samples while the bars estimate the standard error associated with each particle size class.

To quantitatively present the particle size statistics for the combined aerosol instruments, a log-normal particle size distribution was assumed and fitted to the ultrafine and coarse modes in the experimental data (Fig. 2a–g and Table 1). In presenting number statistics for the ultrafine mode, the data obtained by the SMPS/NDMA were used for fitting the left-hand side of this mode as this instrument was optimized to sample aerosols in the particle size range 10–100 nm. In presenting number statistics for the coarse mode, the data obtained by the APS were fitted using the right-hand side of this mode. As can be seen, the

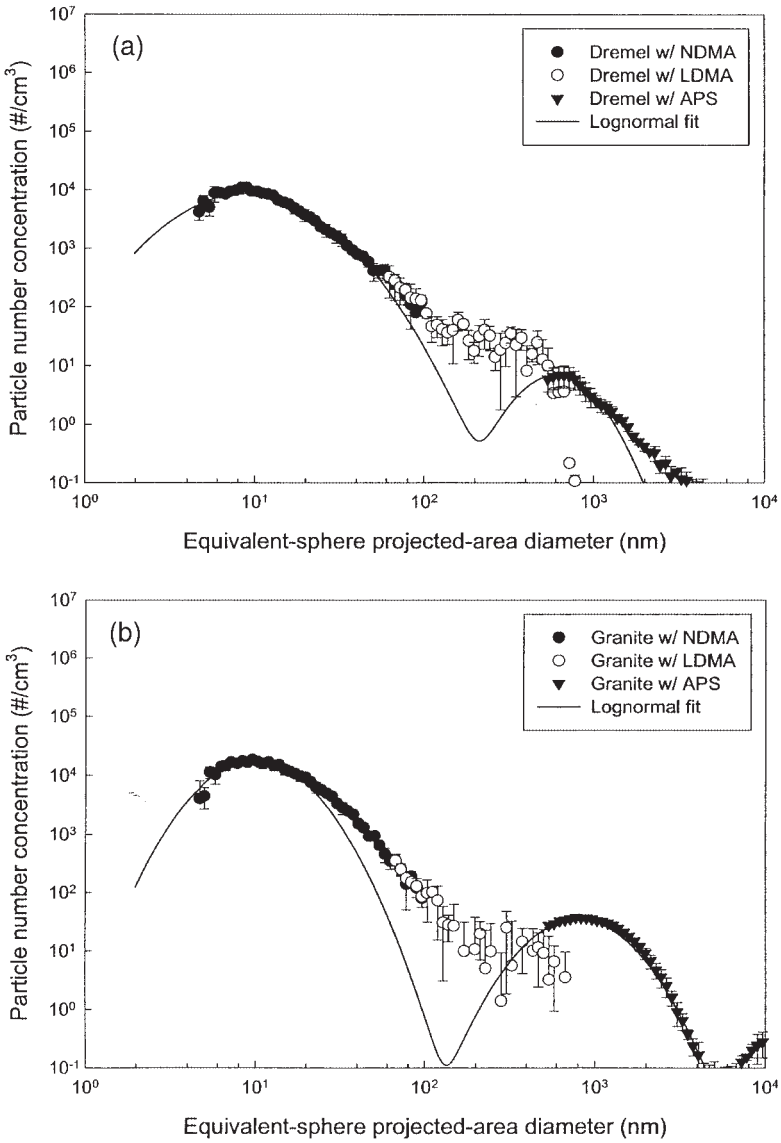

Fig. 2. Variation in particle number concentration [dN/d log(d_p)] as a function of equivalent-sphere projected surface area diameter for (a) the Dremel™ tool without a grinding substrate, (b) a granite substrate, (c) a clay ceramic substrate, (d) a steel substrate, (e) an aluminum substrate, (f) a PTFE substrate and (g) a hardwood substrate using the SMPS/NDMA (solid circles), SMPS/LDMA (hollow circles) and APS (solid triangles). Note that (i) the solid line for each experimental condition represents a log-normal fit of the experimental data, (ii) the error bars represent the standard error associated with three randomized replicate samples and (iii) the experimental data for all substrates have been background corrected for the Dremel™ tool aerosols.

SMPS/LDMA tended to sample particle sizes corresponding to aerosols located between the ultrafine and coarse modes. Sampling errors associated with this instrument tended to be larger than those associated with either of the other instruments above 200 nm, reflecting the low particle detection rate within the instrument in this regime.

The particle size distribution produced by the Dremel™ tool alone (Fig. 2a) appears to be slightly bimodal. In the overlap regions there was relatively good agreement among the aerosol instruments. Grinding upon the granite substrate gave a distribution that was relatively bimodal (Fig. 2b). TEM analysis indicated a large number of particles >1 μm in diameter, characterized by compact non-spherical particles with sharp edges indicative of generation through abrasive removal (Fig. 3a). The micrograph also revealed evidence of large numbers of nanometer size particles on the substrate, although it is not clear whether these originated from the granite substrate or the grinding tool itself.

Grinding of clay ceramic led to a distinct bimodal particle size distribution (Fig. 2c). Some discrepancy was observed in the overlap region between the

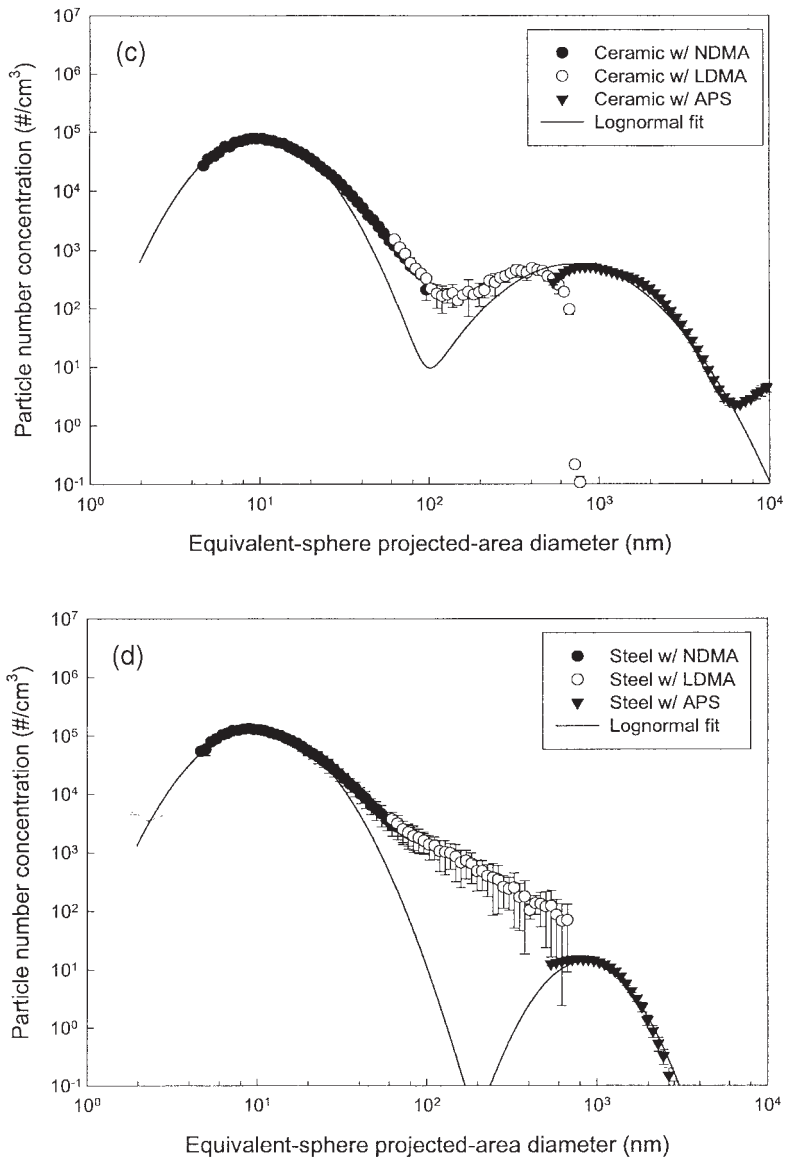

Fig. 2. *Continued.*

APS and the SMPS/LDMA. Both instruments showed decreased detection efficiency for particles in the region of 500 nm and it is likely that this was the source of the observed mismatch. Interpolation between data points below 400 nm and above 800 nm gave a smooth distribution. TEM images were characterized by large numbers of compact particles >1 μm, with some evidence for abraded particles <<1 μm (Fig. 3b).

The aerosol produced when grinding on a steel substrate is shown in Fig. 2d. When compared with the aerosols produced solely by the grinding tool, the total number concentration for this substrate was over one order of magnitude higher, although qualitatively similar to that produced using only the Dremel™ tool (Fig. 2a). Grinding of the steel substrate led to a distinct difference between the results obtained in the overlap region between the SMPS/LDMA and the APS. The high density particles produced from the steel substrate ($\rho \approx 7.9$ kg/m^3), together with uncertainty over their morphology, are probably responsible for the poor transformation between aerodynamic diameter and equivalent-sphere projected area diameter with the APS data. Since the SMPS tends to overestimate particle counts at high diameters when particle counts at lower diameters are significantly higher (an artifact associated with particle residence time within the system), it is conceivable that, in the

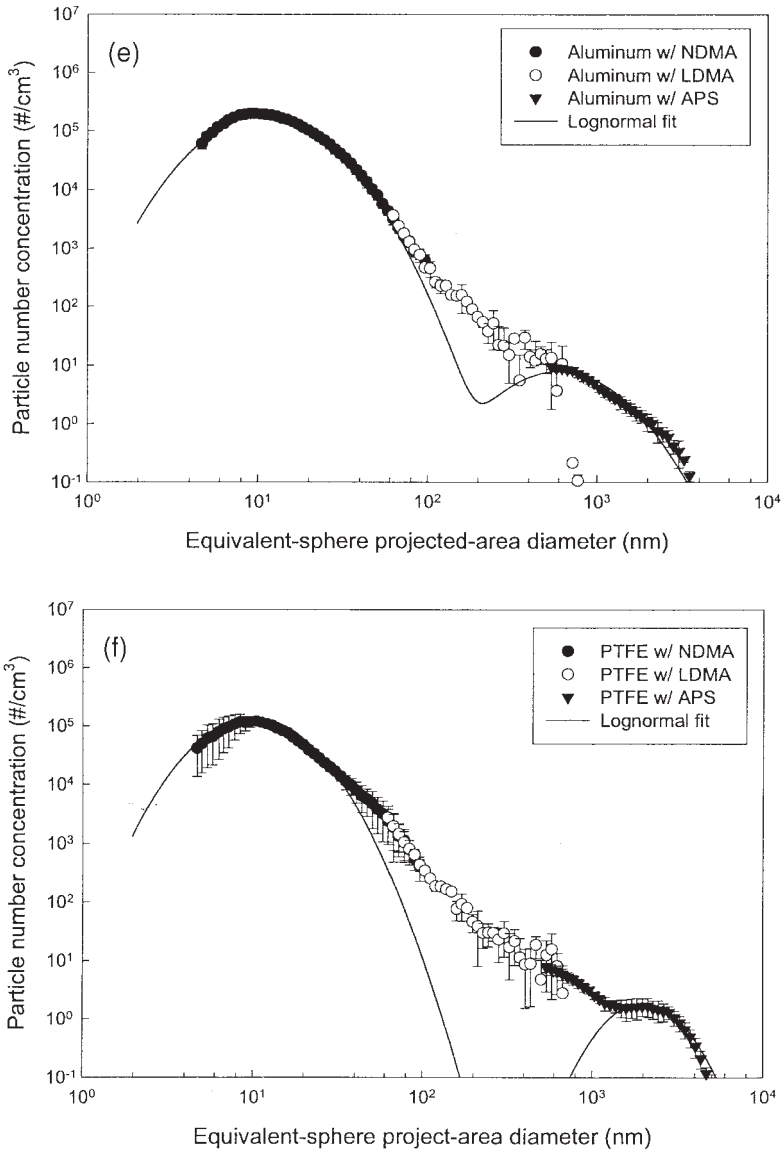

Fig. 2. *Continued.*

absence of such an artifact, better agreement between the SMPS and APS would be seen. In addition, the APS response begins to drop off markedly below ~0.7 μm aerodynamic diameter, corresponding to a physical diameter of ~2 μm with a particle density of ~7.9 kg/m^3. Thus it is likely that the observed mismatch is attributable to instrument response and conversion errors between particle diameters. TEM images were characterized by open chain-like agglomerates of very fine primary particles (Fig. 3c), indicating nucleation followed by growth through coagulation. These images also indicate that many of the particles sampled by the APS may not have been compact (as was assumed).

A similar aerosol size distribution was measured for the aluminum substrate, although no comparable discrepancy between the SMPS/LDMA and APS was seen (Fig. 2e). The behavior of this substrate was qualitatively similar to that produced by the grinding tool itself (Fig. 2a). However, the total number concentration when grinding upon an aluminum substrate was over 18 times higher. TEM images showed large compact particles (Fig. 3d) and many more nanometer size particles. Once again, it was not possible to distinguish a source and generation mechanism for the particles by morphology alone.

The aerosol that resulted from grinding a PTFE substrate is shown in Fig. 2f. Large numbers of single

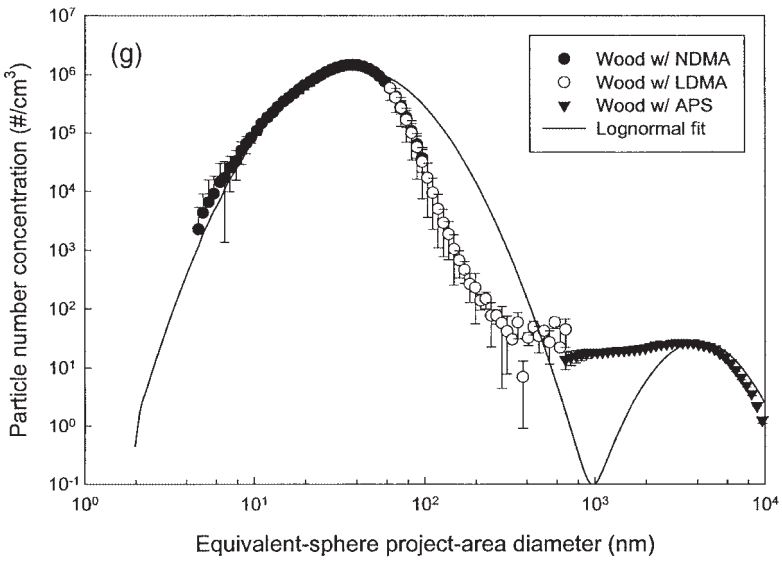

Fig. 2. *Continued.*

particles around 10–20 nm in diameter were seen by TEM (Fig. 3e). Although it was not possible to positively identify these particles, they probably arose from grinding of PTFE because no comparable particles were seen in any of the other samples.

Finally, Fig. 2g shows the measured aerosol size distribution for grinding of oak hardwood. While still bimodal, the lower mode occurs at a much higher diameter than for previous substrates (Table 1). When comparing the instrument response in the overlap region between the SMPS/LDMA and the APS, a distinct difference was noted between the measured results. As in the case of steel, it is likely that uncertainty over the density of the wood-related aerosol and the particle morphology were responsible for a poor transformation between particle aerodynamic diameter and equivalent-sphere projected area diameter. The aerosol collected for TEM was, for the most part, too beam sensitive to allow imaging. The lack of non-organic carbonaceous particles indicated that most of the ultrafine aerosol was associated with incomplete combustion and probably contained a large number of volatile components that evaporated in the TEM.

DISCUSSION

The aerosol number concentrations generated by the Dremel™ tool on the substrates tested varied greatly (Table 1). The particle size distributions tended to be bimodal, with many substrates showing distinct ultrafine and coarse modes. In the overlap region between the SMPS/NDMA and SMPS/LDMA, there was good agreement between the experimental results, demonstrating the usefulness of using the two SMPSs in parallel to measure the particle sizes from 5 to 700 nm. In the overlap region between the SMPD/LDMA and APS, the visual agreement of the size distributions obtained with the two instruments was reasonably good following transformation of aerodynamic diameter to an estimated equivalent-sphere projected area diameter, and only varied appreciably for substrates of very high or low density.

When comparing the particle size distributions for the various substrates, it appears that the coarse modes varied markedly (Fig. 4). Grinding upon a surface such as ceramic or granite produced an aerosol with appreciable number concentrations and a distinct mode, while grinding upon surfaces such as aluminum produced low particle number concentrations and an indistinct mode. Additionally, it appears that the count median particle diameters varied markedly from substrate to substrate, with no discernable pattern.

When viewing all of the substrates together for particle diameters corresponding to the ultrafine mode, it can be seen that, with the exception of wood, the size distributions generated by grinding were qualitatively similar to that produced using the grinding tool alone (Fig. 5). Examining the electron micrographs from each substrate gave little indication of whether particles in the ultrafine mode were primarily associated with the substrate or the carbon brush motor within the grinding tool. Grinding of PTFE was the main exception; this produced large numbers of nanometer diameter, nearly spherical particles that were almost certainly PTFE. Also, micrographs from the steel substrate showed the existence of nanometer size primary particles within large open agglomerates. However, for the aluminum, ceramic and granite substrates the source(s) of the

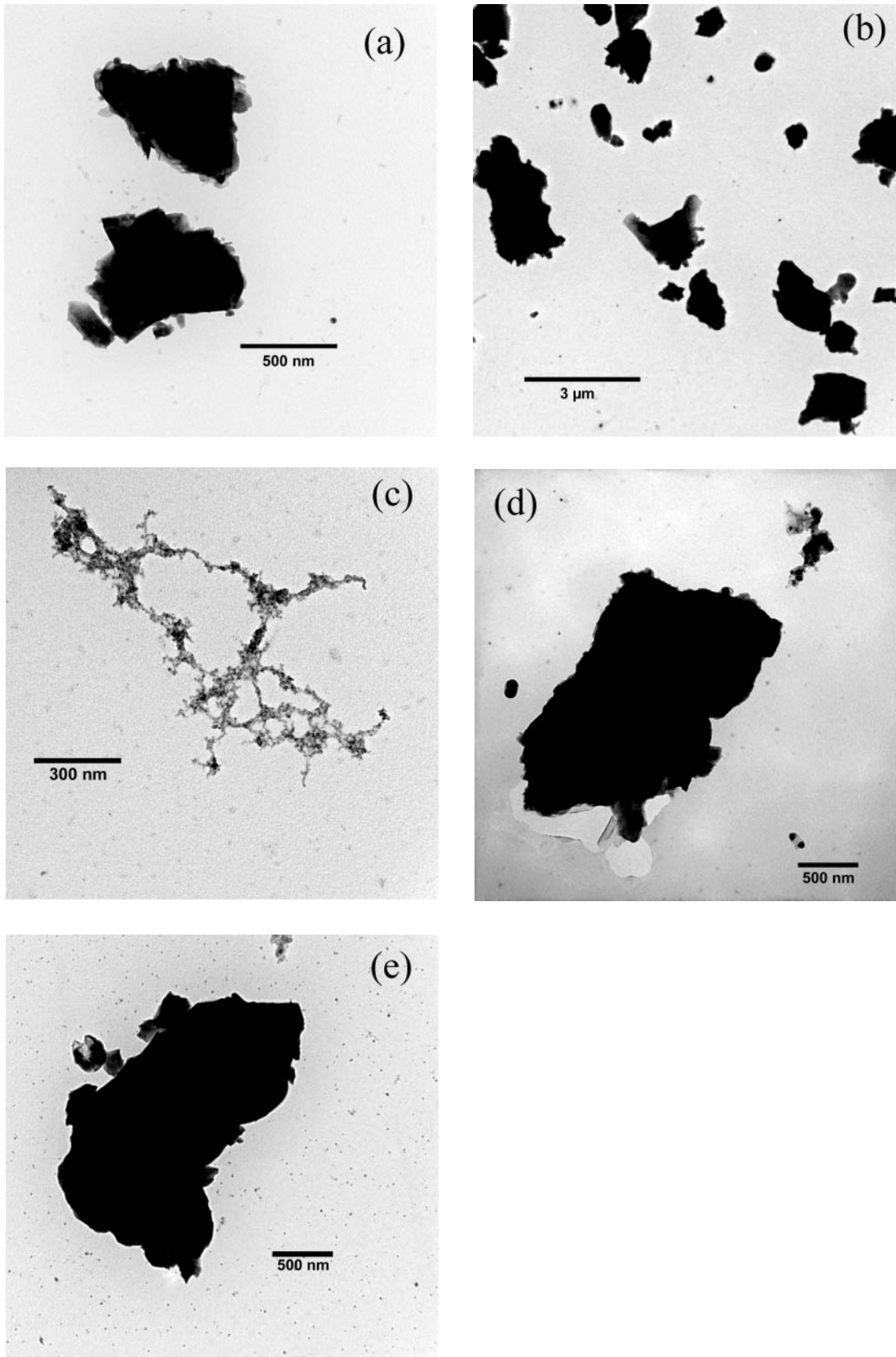

Fig. 3. Transmission electron microscope micrographs of the various grinding substrates including: (a) granite, (b) clay ceramic, (c) steel, (d) aluminum and (e) PTFE. Note that the hardwood TEM sample did not image well, indicating aerosols composed of volatile organic hydrocarbons.

Table 1. Size distribution statistics weighted by particle number for the Dremel™ tool operating by itself and when grinding upon various substrates

Experimental condition	Ultrafine mode			Coarse mode		
	N_{tot} (cm^{-3})	d_{CMD} (nm)	σ_g	N_{tot} (cm^{-3})	d_{CMD} (nm)	σ_g
Dremel™ without substrate	6.5×10^3	9	2.0	3.0×10^0	600	1.5
Granite	1.0×10^4	10	1.7	1.9×10^1	800	1.7
Ceramic	5.0×10^4	10	1.7	4.0×10^2	700	1.9
Steel	8.0×10^4	10	1.7	6.0×10^0	850	1.5
Aluminum	1.2×10^5	11	1.8	5.0×10^0	600	1.8
PTFE	8.0×10^4	10	1.7	8.5×10^{-1}	2000	1.5
Hardwood	8.0×10^5	35	1.7	1.2×10^1	3800	1.5

Particle statistics represent average values for three replicate sample runs and the reported statistics for each substrate have been background corrected.

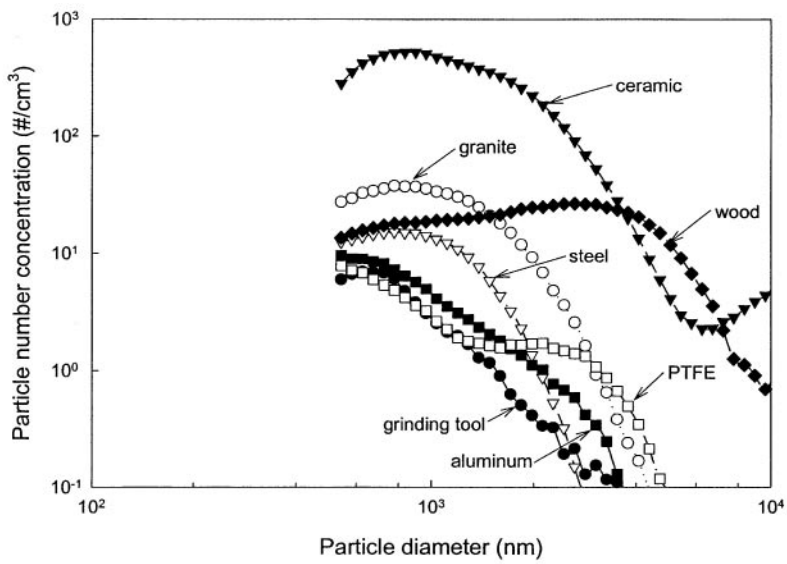

Fig. 4. Composite of the coarse mode experimental results for the Dremel™ tool and various grinding substrates. The information is extracted from Fig. 2a–g.

nanometer size particles could not be discerned. In the case of PTFE and steel, the ultrafine particle morphology indicates formation through nucleation, suggesting that temperatures were sufficiently high at the grinding interface to lead to vaporization or combustion of the substrate. Grinding on wood resulted in an ultrafine aerosol with a markedly larger median diameter and substantially higher number concentration. It showed evidence of charring at the grinding interface, supporting the hypothesis that frictional heating during grinding can lead to the formation of ultrafine particles.

Clearly, a better indicator of the source of an ultrafine particle would be obtained through single particle elemental analysis. Energy dispersive X-ray analysis (EDX) is widely used in transmission electron microscopy to identify elemental composition. However, when applied to nanometer sized particles EDX is limited by long sample collection times and the sensitivity of the sample to beam damage and contamination. In this case, it was not possible to obtain meaningful information from the samples using EDX. For a better understanding of the source of the ultrafine mode arising from grinding on these substrates, the use of alternative sample collection methods or analytical methods such as electron energy loss spectroscopy (EELS) should be considered for future research (Brydson, 2000; Maynard, 2000).

Although these data raise some ambiguity over the source of the ultrafine particles, they also raise the question of whether the process leading to mechanical aerosol generation should be considered a source of particles in its own right. A number of publications have indicated that for low solubility, chemically 'inert' materials the composition of ultrafine particles is of secondary importance (Oberdorster *et al.*, 1995; Donaldson *et al.*, 1998; Brown *et al.*, 2001). If this is

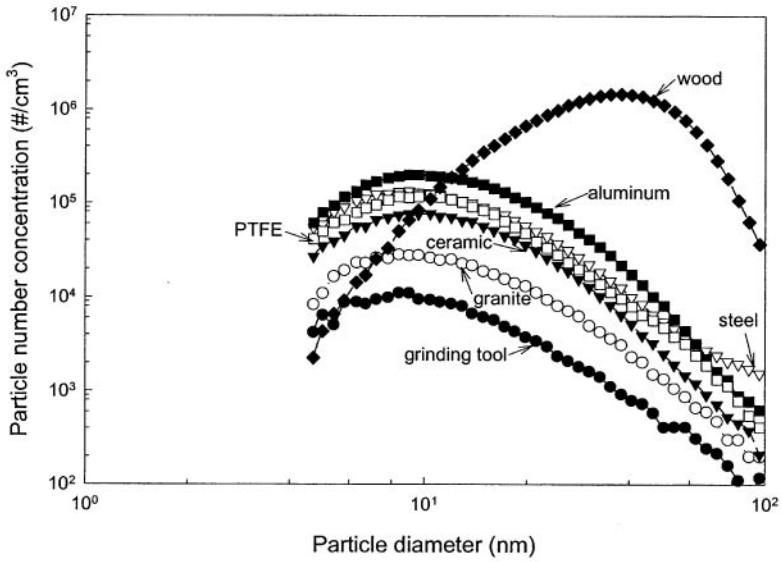

Fig. 5. Composite of the ultrafine mode experimental results for the Dremel™ tool and various grinding substrates. The information is extracted from Fig. 2a–g.

the case, there is little to be gained in differentiating between particles generated by the tool and those from the substrate. However, in the case of highly toxic particles such as silica, it would be important to differentiate between the aerosols generated by these two sources. Clearly, there is further research to be carried out in this area.

CONCLUSIONS

In this preliminary study of particle formation upon high-speed grinding we have shown that ultrafine particles are generated by a variety of substrates. There is evidence that grinding of some substrates produced ultrafine particles through vaporization or combustion of the substrate material. In the absence of a substrate, there was also evidence that the grinding tool led to the formation of ultrafine particles, albeit at a much lower concentration. Further research into the chemical nature of individual particles is required to elucidate the relative source contributions during grinding operations.

REFERENCES

ACGIH. (1990) Threshold limit values for chemical substances and physical agents. Cincinnati, OH: American Conference of Governmental Industrial Hygienists.

Brown DM, Wilson MR, MacNee W, Stone V, Donaldson K. (2001) Size-dependent proinflammatory effects of ultrafine polystyrene particles: a role for surface area and oxidative stress in the enhanced activity of ultrafines. Toxicol Appl Pharmacol; 175: 191–9.

Brydson R. (2000) A brief review of quantitative aspects of electron energy loss spectroscopy and imaging. Mater Sci Technol; 16: 1187–98.

Cheng Y-S, Yeh H-C, Kanapilly GM. (1981) Collection efficiencies of a point-to-plane electrostatic precipitator. Am Ind Hyg Assoc J; 42: 559–632.

Choe KT, Trunov M, Grinshpun SA *et al.* (2000) Particle settling after lead-based paint abatement work and clearance waiting period. Am Ind Hyg Assoc J; 61: 798–807.

Donaldson K, Li XY, MacNee W. (1998) Ultrafine (nanometer) particle mediated lung injury. J Aerosol Sci; 29: 553–60.

Kinney PD, Pui DYH. (1995) Inlet efficiency study for the TSI Aerodynamic Particle Sizer. Part Part Syst Char; 12: 188–93.

Kusaka Y, Kumagai S, Kyono H, Kohyama N, Shirakawa T. (1992) Determination of exposure of cobalt and nickel in the atmosphere in the hard metal industry. Ann Occup Hyg; 36: 597–607.

Lehmann E, Frohlich N. (1988) Particle size distribution of wood dust at the workplace. J Aerosol Sci; 19: 1433–5.

Maynard AD. (2000) Overview of methods for analysing ultrafine particles. Phil Trans R Soc A; 358: 2593–609.

McCawley MA, Kent MS, Berakis MT. (2001) Ultrafine beryllium number concentration as a possible metric for chronic beryllium disease risk. Appl Occup Environ Hyg; 16: 631–8.

NIOSH. (1992) Recommendations for occupational safety and health: compendium of policy documents and statements. Cincinnati, OH: National Institute for Occupational Safety and Health.

Oberdorster G, Gelein RM, Ferin J, Weiss B. (1995) Association of particulate air pollution and acute mortality: involvement of ultrafine particles? Inhal Toxicol; 7: 111–24.

OSHA. (1997) OSHA Table Z-1-A. Washington, DC: Occupational Safety and Health Administration.

Rogak SN, Flagan RC, Nguyen HV. (1993) The mobility and structure of aerosol agglomerates. Aerosol Sci Technol; 18: 25–48.

Thorpe A, Brown RC. (1994) Measurements of the effectiveness of dust extraction systems of hand sanders used on wood. Ann Occup Hyg; 38: 279–302.